Proceedings of the 5th International Conference on Civil Engineering for Sustainable Development (ICCESD 2020), 7~9 February 2020, KUET, Khulna, Bangladesh (ISBN-978-984-34-8764-3)

ANALYTICAL MODELING FOR CONSTITUTIVE RELATIONSHIP OF ULTRA-HIGH-PERFORMANCE FIBER REINFORCED CONCRETE WITH VARYING SIZES

Arafat Alam*[1] and Md. Habibur Rahman Sobuz[2]

[1]Undergraduate Student, Department of Building Engineering and Construction Management, Khulna University of Engineering and Technology, Bangladesh, e-mail: arafat.alam1892@gmail.com
[2]Assistant Professor, Department of Building Engineering and Construction Management, Khulna University of Engineering and Technology, Bangladesh, e-mail: habib@becm.kuet.ac.bd

***Corresponding Author**

ABSTRACT

In modern construction, ultra-high-performance fiber-reinforced (UHPFRC) concrete plays a pivotal role by significantly increasing strength and ductility. Application of UHPFRC ranges vast, from bridges to high-rise structures. In this research, the primary focus is on the size-dependent analytical constitutive relationship of UHPFRC of varying heights. The model was then verified with the prior experimental data. The experimental part involves the testing of cylinders with three different volume of fiber contents of 1 %, 2%, and 3%. The heights of the cylindrical specimen were also varied by 200mm, 300mm and 400mm heights and having a fixed diameter of 100 mm. The analytical constitutive relationship was numerically approximated based on empirical equations proposed by Popovics. A regression analysis was carried out which resulted into equations for peak strain of different fiber-volume and these equations are then incorporated into the model to predict stress-strain relationships from one size to any other sizes. Finally, the model, was validated with the experimental data. It is observed that the model can predicts the stress-strain relationship in a rather conservative way. Thus, it is concluded that there exists a correlation between the stress-strain of UHPFRC concrete and the varying sizes of the specimen.

Keywords: *UHPFRC; Size-dependent behavior; Stress-strain response; Fiber content; Ductility.*

1. INTRODUCTION

Ultra-high-performance concrete (UHPC) is a relatively new class of concrete that transcends typical compressive, tensile and durability behavior of normal weight concrete (B. A. Graybeal, 2007). UHPC is a new-generation high mechanical performant cementitious matrix material (Pierre Richard, 1995). UHPC mainly overcomes the weakness of concrete strength and brittleness and shows high strength and post-cracking tensile strength (Shafieifar, Farzad, & Azizinamini, 2017; Sobuz et al., 2016). But to achieve UHPC, unorthodox mix design by mixing Portland cement, fine sand, silica fume, ground quartz, superplasticizers, steel or organic fibers and water with low w/c ratio of typically less than 0.25 is applied (B.A. Graybeal, 2003). Coarse aggregate is reduced in this type of concrete, which in turn reduces the size of microcracks and thus using reactive powder, the concrete may have compressive strength ranging from 200MPa to 800MPa (Pierre Richard, 1995). Even without complex mixing, research has shown that compressive strength in the range of 130-160 MPa is achievable using only conventional materials (Sobuz et al., 2016). Applications of UHPC can be architectural and structural but it is most favorable for bridge construction and precast construction for its life-cycle cost (B.A. Graybeal, 2003). The inclusion of steel fibers in UHPC opens up the door for Ultra-high-Performance Fiber-Reinforced Concrete(UHPFRC), which shows improved elastic modulus, tensile strength, elastic post-cracking bending strength and ductility*(*Toledo Filho, Koenders, Formagini, & Fairbairn, 2012*)*.Graybeal has maintained that UHPC shows enhanced durability due to the discontinuous pore structure (B.A. Graybeal, 2003). Normal weight concrete exhibits lower post-peak strength and shorter strain time and fails in sudden explosive behavior but UHPFRC exhibit higher post-peak strength, longer strain time and due to the integrated fiber and matrix bonding, even in the failure the surface remains intact (Shafieifar et al., 2017). Different fibers with a good elastic property are seen to enhance the durability of UHPFRC. Ductility is the phenomenon of undergoing large deformation before failure, and it is important as it provides a warning prior to structural failure. Yoo et al conducted biaxial flexural performance of UHPFRC with three different fiber lengths and two placement methods of which, the result was higher load-carrying and deflection capacity with longer fiber length (Yoo & Yoon, 2016). Considering the type of steel fiber, previous research shows that twisted steel fibers improve both post-peak tensile strength and ductility capacities (Kim, 2011; Wille K, 2014). Lubell et al conducted in his experiment, as the fiber volume fraction increased, peak strengths and post-peak ductility in compression, flexure, and direct shear also increased. This phenomenon is explained as steel fibers partially restraining the lateral expansion and enabling larger axial deformation. Lubell et al also showed in his research that the ascending branch has a linear slope which is independent of fiber content (Kazemi & Lubell, 2012).

Size-dependency is another factor that controls the stress-strain properties of concrete in addition to material mixing. The same materials with different shapes and sizes produce different stress-strain behavior (Chen, Visintin, Oehlers, & Alengaram, 2014). Research has shown that size and shapes directly control the compressive strength of concrete specimens *(*Frettlöhr, H. Reineck, & W. Reinhardt, 2012*;* Lubell*;* Pierre-Claude Aitcin, 1994*;* YI, 2002*)*. With the increase in size, length or depth, compressive strength, and ductility reduce significantly (Mindessb). These research shows that other material properties such as axial tension, flexure, combined bending and axial forces, Elastic limits, Tensile stresses also show anomaly with different specimen sizes. Cube specimens have slightly higher compressive strength than the same mixing cylinders, but in stages of higher compressive strength, the strength difference declines. For the softening branch, cube shows a milder slope while cylinder shows a steeper slope (del Viso, Carmona, & Ruiz, 2008). There has been no accurate relationship established between the peak compressive strength of cylinder and cube samples of different sizes for various volume fractions (Davis, 2008). Implementation of the UHPC has not produced the expected impact due to a lack of material and production knowledge and high costs. (Maher KT, 2016). Analytical methods for stress-strain determination can mitigate these problems. Popovic, Carreira and Chu, Neville, Wee et al are some of those researchers who have proposed empirically-based numerical approximations for stress-strain behavior of particular concretes (Ayub, 2014; Popovics, 1973). But, as of now, there is not any equation pertaining to the prediction of the stress-strain behavior of UHPFRC (B. A. Graybeal, 2007). A numerical model predicting stress-strain behavior of UHPFRC which also accounts for size-dependency characteristics will accelerate knowledge gaining on UHPFRC. Chen et

al, in his paper, focused on the importance of wedge sliding from the shear-friction mechanism which varies with shape and to measure the global strain of a specimen, wedge sliding is necessary to quantify. Then he proposed a stress-strain relationship for normal-weight concrete (NWC) which is shape and size-dependent and can be used to derive various stress-strain models from one fixed-sized stress-strain data.

This study predicts and compares the size-dependency characteristics of UHPFRC with experimental data. The experimental tests are done to create UHPFRC with different fiber volume content and specimen sizes. The varying height incorporates the size-dependency characteristics of UHPFRC, and varying percentages of fiber are done to evaluate the fiber-effect on the compressive strength of UHPFRC with varying height. Popovics's stress-strain model is then corrected with size-dependency formulation as suggested by Chen et al. Using the model, different heights (size) and volume-fraction fiber content specimens are modeled numerically to compare with the experimental data to study the effect of size and fiber-content in both experimental and numerical model.

2. METHODOLOGY

2.1.1 Analytical Investigation

Nonlinear analysis is the primary method for analyzing compression failure of structural members and for nonlinear analysis, the complete stress-strain curve of the unconfined concrete is necessary (Zhao-Hui Lu and Yan-Gang Zhao). To predict the stress-strain curve of particular concrete, an enormous amount of experimental and theoretical research has been conducted and many researchers have proposed empirically-based numerical approximations for this matter (Lu & Zhao, 2010; Mansur, Chin, & Wee, 1999; Popovics, 1973). However, due to concrete being a mixture of different materials and without a uniform mix design, there is no universal consensus equation available (B. A. Graybeal, 2007). Moreover, there is not any equation available which can generally predict the stress-strain curve of UHPFRC (B. A. Graybeal, 2007).

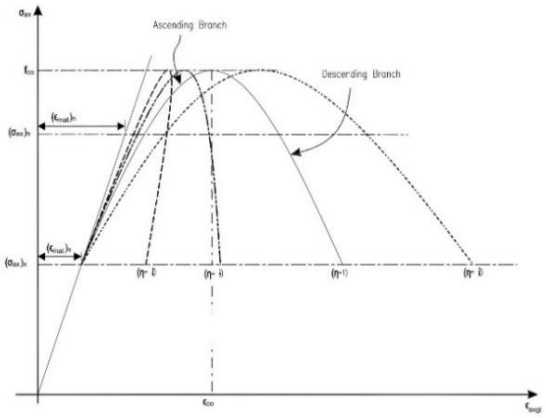

Figure 1: Size-Dependent σ_{ax}- ε_{axgl} from Chen. et. al (2014)

The size-dependency of concrete specimens is important as different sized specimen produce different results (Kazemi & Lubell, 2012). From global strain (ε_{axgl}) it is possible to understand the size-effect on stress-strain relationship of a specimen. Chen et al. (Chen et al., 2014) suggested an equation for global stress-strain,

$$(\varepsilon_{axgl-2})_n = [(\varepsilon_{axgl-1})_n - (\varepsilon_{mat})_n]\frac{L_{pr-1}}{L_{pr-2}} + (\varepsilon_{mat})_n \quad (1)$$

In equation (1), ε_{axgl-1} is the global strain of a standard cylinder of 200 mm and L_{pr-1} is the specific length of that, ε_{mat} is the material strain and L_{pr-2} is the specific length of the required specimen. The subscript η is the size factor equivalent to L_{pr-1}/L_{pr-2}. Fig 1 illustrates the diagram of the equation for the stress level $(\sigma_{ax})_n$. It can be seen that up to $(\sigma_{ax})_x$, every specimen has same material strain and the ascending

branch has a similar linear slope for every specimen. Test stress-strain relationship for η =1 is used as a base to plot other stress-strain relationships for different lengths L_{pr-2}. Figure 1 illustrates that as the η reduces, reduction in ductility in the descending branch is apparent and contrary, as the η increases, an increase in ductility in the descending branch is seen. Moreover, fig 1 also illustrates the ductile behavior of UHPC – it shows considerable residual stress even in higher strain after reaching peak strain.

To make the existing peak strain-based stress-strain relationships size-dependent, Chen et al proposed an adjusted value of $\boldsymbol{\varepsilon_{co}}$ for size-dependency characteristics (Chen et al., 2014). This adjusted $\boldsymbol{\varepsilon_{co}}$ strain makes the stress-strain size-dependent and stress-strain relationship for any size can be derived from one standard size. While using this equation, the slenderness factor **μ** has to be equal to or more than 2. Here, **μ** is the ratio of length to diameter for cylinder specimen. Graybeal et al conducted in his paper that the increase in the size of fiber-reinforced concrete significantly reduces the compressive strength (B. A. Graybeal, 2007). But there is not any existing consensus equation that can predict size-dependent stress-strain behavior of UHPFRC. Previous researches have shown that fiber significantly improves post-peak behavior and enhances strain characteristics of concrete in both compression and tension (Dwarakanath & Nagaraj, 1991; Nataraja, Dhang, & Gupta, 1999).

2.1.2 Popovics's Model (1973)

The model proposed by Popovics can estimate the complete stress-strain diagram of concrete. This model predicts both the ascending and descending branches of the stress-strain curve.

$$f = f_0 \frac{\varepsilon}{\varepsilon_0} \frac{n}{n-1+\left(\varepsilon/\varepsilon_0\right)^2} \tag{2}$$

This model predicts good stress-strain behavior for up to 69 MPa concrete. For incorporating size-depending behavior, Chen et al have modified the Popovics's equation by replacing peak strain (ε_o) with an adjusted peak strain (ε_{co}) and n with r , which is a factor that controls the ductility of the concrete, and $r = \frac{E_c}{[E_c-(f_{co}/\varepsilon_{co})]}$. Chen et al used regression analysis on test results of normal weight concrete for the value of ε_o.

Thus, the modified Popovics's formula for the size-dependent stress-strain diagram is,

$$f = f_{co} \frac{\left[\frac{(\varepsilon ax)pop}{\varepsilon co}\right] r}{r-1+\left[\frac{(\varepsilon ax)pop}{\varepsilon co}\right]^r} \tag{3}$$

This yields the size-dependent stress-strain relationship for Popovics's equation. The authors in this study have conducted regression analysis for deriving Chen's moderated factors (ε_{co}**)** for three different fiber-volume content of UHPFRC and incorporated the factors in previously proposed Popovics's analytical model equation (2) to propose a size-dependent stress-strain model of UHPFRC.

2.1.3 Extracting Regression

Global strain at peak stress (f_{co}) for a specimen of length 200 mm, $\boldsymbol{\varepsilon_{co\text{-}200}}$, can be utilized to formulate size-dependent characteristics for the predictive model. Peak strain can be converted into global strain for a specimen of length 200 mm by using Chen's equation-(Chen et al., 2014),

$$\varepsilon_{co-200} = \left(\varepsilon_{co-test} - \frac{f_{co}}{Ec}\right) \frac{L_{pr-test}}{200} + \frac{f_{co}}{Ec} \tag{4}$$

Where,

f_{co} = Peak stress

$\boldsymbol{\varepsilon_{co\text{-}test}}$ = Peak strain from test result

$L_{pr\text{-}test}$ = Length of test specimen

$L_{pr\text{-}200}$ = Test specimen length converted to 200 mm

The authors have performed linear regression on 121 published test results pertaining to the relevant topic (Al-Azzawi & Sarsam, 2010; Bencardino, Rizzuti, & Spadea, 2007; Bencardino, Rizzuti, Spadea, & Swamy, 2008; Bhargava, Sharma, & Kaushik, 2006; Earle, Bowden, & Guy; Graybeal, 2005; B. Graybeal, 2007; Jiao, Sun, Huan, & Jiang, 2009; Jo, Shon, & Kim, 2001; Lavanya, Dattatreya, M.Neelamegam, & Seshagiri Rao, 2010; Lavanya, J K, & Neelamegam, 2014; Lee; Mansur et al., 1999; Suksawang, Wtaife, & Alsabbagh, 2018) to determine relationships between $\boldsymbol{\varepsilon_{co\text{-}200}}$ and $f_{co.}$. Later, the authors have divided the test results by 3 different volume percentages of steel fibers – 1%, 2%, and 3% and performed linear regression for the aforementioned percentages with test results of a similar percentage of steel fiber. For 1% fiber-volume content, the linear regression gave the following equation relationships between $\varepsilon_{co\text{-}200}$ and $f_{co,}$

$$\varepsilon_{co-200} = 6.42 \times 10^{-6} f_{co} + 2.88 \times 10^{-3} \quad (5)$$

For 2%, the linear regression gave the following equation relationships between $\boldsymbol{\varepsilon_{co\text{-}200}}$ and $f_{co,}$

$$\varepsilon_{co-200} = -1.78 \times 10^{-6} f_{co} + 3.88 \times 10^{-3} \quad (6)$$

For 3%, the linear regression gave the following equation relationships between $\boldsymbol{\varepsilon_{co\text{-}200}}$ and $f_{co,}$

$$\varepsilon_{co-200} = 1.08 \times 10^{-6} f_{co} + 3.44 \times 10^{-3} \quad (7)$$

The model will incorporate equations (4-7) to produce an estimate for size-dependent stress-strain curves for UHPFRC.

2.2 Experimental Test Specification

The experimental test was initiated to investigate the size-dependent compressive strength and stress-strain behavior of UHPFRC. Two major influencing factors in preparing test specimens are – Varying fiber volume-content and size of the specimen. For each fiber content from 1% to 3%, size-wise three types of cylinder, with a fixed diameter of 100 mm and varying height 200 mm, 300 mm and 400 mm were cast. To get a more accurate result, for each type of cylinders, 3 cylinders were cast and the mean value was used in the paper.

The mix composition was adopted from the previous work (Sobuz et al., 2016). One commercially available fiber – Dramix 4D was used and are available from Bekaet Ltd in South Australia. All of the steel fibers were hooked end wired type. The compression strength tests were carried out according to the standard (ASTM-C39/C39M-12, 2012). An Amsler Compressive Testing Machine with a maximum capacity of 5000 kN was used to determine stress-strain behavior. Load control was the controlling measure up to the peak strength and after that, the specimens were under deflection control. The loads were applied on the top surface of 100 mm diameter cylinders. The load application rate was maintained at 50 kN/min in the ascending branch. After the peak load, for the descending branch, the displacement was at 0.1 mm/min. At day 56, 4 LVDTs were equipped to measure the total platen to platen axial deformation and 3 LVDTs equally spaced laterally at mid-height were equipped to measure the total lateral dilation. For measuring axial strain due to concentric load, two axial gauges were used and for lateral strain, three lateral strain gauges were used.

3. EXPERIMENTAL TEST RESULTS

Axial stress-strain results involving peak strength, peak strain, failure strength and failure strain of different fiber content are presented in Table 1. Predominantly, it can be seen from Table 1 that, the strength ranges from 137 MPa to 160 MPa with corresponding peak strain .004156 to .004515 for test series 1, strength ranges from 124 MPa to 142 MPa with corresponding peak strain 0.003544 to 0.003708 for test series 2 and strength ranges from 140 MPa to 143 MPa with corresponding peak strain 0.004027 to 0.004389 for test series 3.

Table 1: UHPFRC experimental test result

Specimen Designation	Test Series	Fiber %	Peak Strength (MPa)	Peak Strain	Failure Strength (MPa)	Failure Strain
S-100x200-1	1	1	137	0.004156	6.683	0.101
S-100x200-2	1	2	155	0.004437	4.394	0.148
S-100x200-3	1	3	160	0.004515	7.234	0.187
S-100x300-1	2	1	124	0.003544	0.6288	0.0923
S-100x300-2	2	2	142	0.003664	2.476	0.1098
S-100x300-3	2	3	142	0.003708	1.469	0.1322
S-100x400-1	3	1	140	0.004027	0.981	0.0660
S-100x400-2	3	2	142	0.003963	1.948	0.0797
S-100x400-3	3	3	143	0.004389	2.819	0.0918

It is noted that the highest peak strength observed was 160 MPa for S-100x200-3 specimen and the highest peak strain was 0.004515 for S-100x200-3 specimen. It satisfies that with the introduction of higher fiber content, the peak strain and failure strain increases significantly for each size.

From table 1, it can be seen that failure strain for UHPFRC is significantly higher than normal-weight concrete at higher strain. For NWC, the failure strain is in the vicinity of 0.005 whereas, for UHPFRC, the lowest failure strain observed in the experiment is 0.0660 (Lim & Ozbakkaloglu, 2014). This phenomenon indicates that serviceability for UHPFRC is significantly higher than NWC and exhibits more ductile behavior

4. ANALYTICAL RESULTS

It is possible to predict stress-strain behavior for other lengths of specimen after testing one standard specimen length. After selecting a standard length of specimen, equation (4) can be applied to convert other specimen lengths to the standard one. This way the global strain for standard $\boldsymbol{\varepsilon_{co\text{-}standard}}$ can be converted into global strain for other length $\boldsymbol{\varepsilon_{co\text{-}others}}$**.** For instance, global strain for $\mathbf{L_{pr\text{-}200}}$ is $\boldsymbol{\varepsilon_{co\text{-}200}}$**,** which can be converted into $\boldsymbol{\varepsilon_{co\text{-}300}}$ for specimen length of 300 mm and likewise.

For this study, the authors have used three base specimen sizes for three different fiber-volume percentages to predict stress-strain behavior of other sizes in a similar fiber-volume percentage. For the similar fiber-volume percentage, predicted derived numerical stress-strain behaviors for other specimen sizes are then compared with previous experimental results.

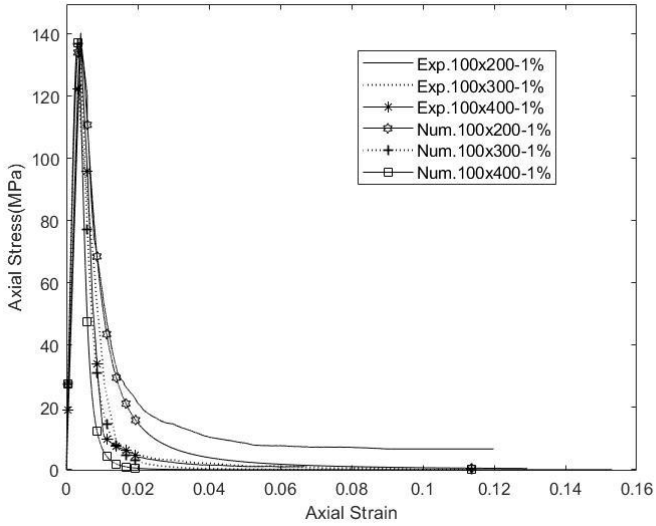

Figure 2: Experimental data vs numerical data for 1% fiber-volume content

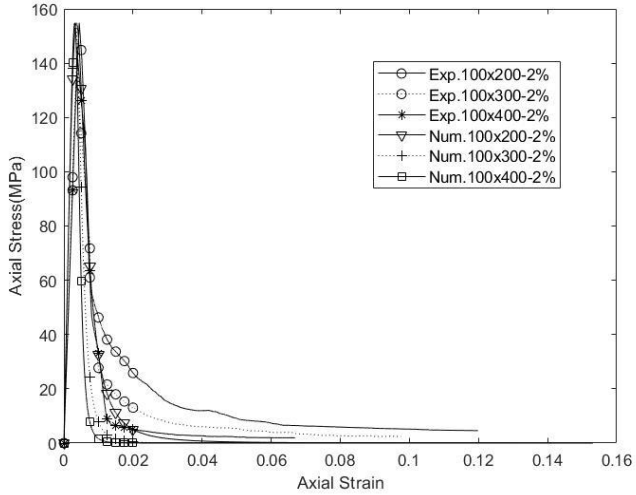

Figure 3: Experimental data vs numerical data for 2% fiber-volume content

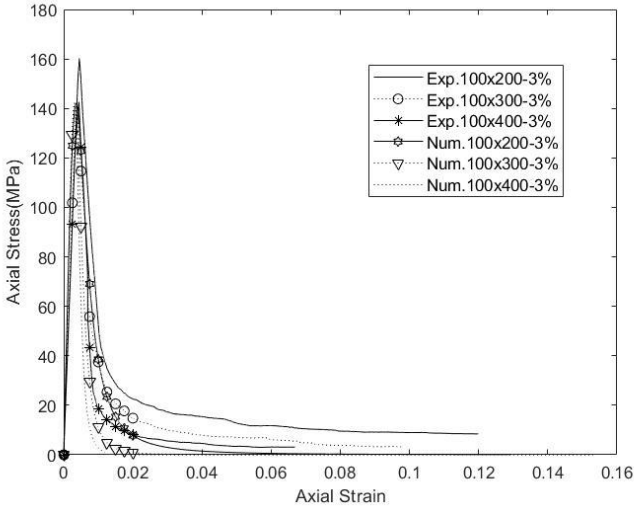

Figure 4: Experimental data vs numerical data for 3% fiber-volume content

For 1%, 100x200 mm is taken as the base size specimen. Numerical behavior of for 100x200 mm, 100x300 mm and 100x400 mm with 1% fiber-volume is derived using equations (4) and (5) which is exhibited in figure 2. Both experimental and numerical stress-strain graph shows linearity till the peak stress. The model accurately predicts linear behavior equivalent to the experimental. The model also predicts compressive peak stress with accuracy. For UHPC, a steep post-peak is observed in both works of literature (Mansur et al., 1999) and in this experimental result. The model closely predicts steep post-peak behavior relative to the experimental post-peak behavior. The specimen exhibits relatively higher residual stress even in higher strain – 100x200 mm exhibits around 36 MPa for a strain of 0.016 and the model is able to predict closely similar residual stress in a similar strain. This indicates the ductility characteristics of UHPFRC; hence, the model is also able to predict the ductility property of UHPFRC.

For 2%, 100x200 mm is taken as a base specimen. Numerical behavior of 100x200 mm, 100x300 mm, and 100x400 mm with 2% fiber-volume is derived using equations (4) and (6) which is shown in figure 3. Figure 3 and figure 4 shows that similar characteristics to 1% can be observed for 2%. With the increase of fiber-volume, compressive strength tends to be higher (Kazemi & Lubell, 2012). In this study, 2% fiber-volume increased compressive strength to 155 MPa for 100x200 mm specimen. The model predicts closely to the increased compressive strength for 2%. Moreover, it is noted that with increased specimen size, lower compressive strength is obtained (Kazemi & Lubell; Lubell). In this study, 100x300 mm and 100x400 mm exhibited lower compressive strength than 100x200 mm and the model is able to predict the drop in compressive strength with increased size. For 3%, a similar procedure was followed and similar results were obtained using equations (4) and (7), which is shown in figure 4. Figure 4 predicts similar correlation – linear behavior, peak stress, steeper post-peak behavior, analogous stress-strain behavior with the influence of specimen-size and ductility property. Thus, the model predicts a conservative estimate with the experimental results.

5. CONCLUSIONS

The study was undertaken to construct a model for estimating size-dependent stress-strain curves for UHPFRC. For establishing the model, using Popovic et al's (Popovics, 1973) equation and Chen et al's (Chen et al., 2014) global strain equation, regression analysis was conducted on 121 published test results to generate size-dependent stress-strain equations for UHPFRC. Three equations were generated for three different fiber-volume contents – 1 %, 2 %, and 3 %. A comparison of the prediction from this model and experimental test data manifests good consistency. The model accurately predicts up to material strain and provides a conservative estimate for the softening branch with the experimental data. Commensurate estimate for softening branch allows future research pertaining to high cyclic load, fatigue, earthquake by utilizing this model. It is possible to estimate any specimen sized stress-strain behaviors using this model just by experimenting with one standard size. As a result, a significant reduction of cost, time and material can be achieved while conducting future research in UHPFRC.

ACKNOWLEDGEMENTS

The authors wish to acknowledge the financial support of the Australian Government Department of Defense's ''Defense Science and Technology Organization". The experimental study was conducted in the Chapman structural laboratory of the School of Civil, Environment and Mining Engineering, The University of Adelaide, South Australia. The numerical modeling part of the research was carried out in the high-speed computers in BIM laboratory in the Department of Building Engineering and Construction Management, Khulna University of Engineering and Technology, Khulna-9203, Bangladesh.

REFERENCES

Al-Azzawi, Z., & Sarsam, K. (2010). Mechanical Properties of High-Strength Fiber Reinforced Concrete. *Engineering and Technology Journal, 28*, 2442.

Ayub, T. (2014). *Stress-Strain Response of High Strength Concrete and Application of the Existing Models* (Vol. 8).

B.A. Graybeal, P. E., J.L. Hartmann, P.E. (2003). *ULTRA-HIGH PERFORMANCE CONCRETE MATERIAL PROPERTIES*. Paper presented at the Transportation Research Board Conference.

Bencardino, F., Rizzuti, L., & Spadea, G. (2007). Experimental tests vs. theoretical modeling for FRC in compression. *Proceedings of the 6th International Conference on Fracture Mechanics of Concrete and Concrete Structures, 3*, 1473-1480.

Bencardino, F., Rizzuti, L., Spadea, G., & Swamy, R. (2008). Stress-Strain Behavior of Steel Fiber-Reinforced Concrete in Compression. *Journal of Materials in Civil Engineering - J MATER CIVIL ENG, 20*. doi:10.1061/(ASCE)0899-1561(2008)20:3(255)

Bhargava, P., Sharma, U. K., & Kaushik, S. (2006). Compressive Stress-Strain Behavior of Small Scale Steel Fibre Reinforced High Strength Concrete Cylinders. *Journal of Advanced Concrete Technology - J ADV CONCR TECHNOL, 4*, 109-121. doi:10.3151/jact.4.109

Chen, Y., Visintin, P., Oehlers, D. J., & Alengaram, U. J. (2014). Size-Dependent Stress-Strain Model for Unconfined Concrete. *Journal of Structural Engineering, 140*(4). doi:10.1061/(asce)st.1943-541x.0000869

Davis, B. G. a. M. (2008). Cylinder or Cube: Strength Testing of 80 to 200 MPa (11.6 to 29 ksi) Ultra-High-Performance Fiber-Reinforced Concrete. *ACI MATERIALS JOURNAL, 105*(6).

del Viso, J. R., Carmona, J. R., & Ruiz, G. (2008). Shape and size effects on the compressive strength of high-strength concrete. *Cement and Concrete Research, 38*(3), 386-395. doi:10.1016/j.cemconres.2007.09.020

Dwarakanath, H. V., & Nagaraj, T. S. (1991). *Comparative study of predictions of flexural strength of steel fiber concrete* (Vol. 88).

Earle, P., Bowden, D., & Guy, M. (2012). Twitter earthquake detection: Earthquake monitoring in a social world. *Annals of geophysics = Annali di geofisica, 54*. doi:10.4401/ag-5364

Frettlöhr, B., H. Reineck, K., & W. Reinhardt, H. (2012). Size and Shape Effect of UHPFRC Prisms Tested under Axial Tension and Bending. In (Vol. 2, pp. 365-372).

Graybeal, B. (2005). Characterization of the behavior of ultra-high performance concrete.

Graybeal, B. (2007). Compressive Behavior of Ultra-High-Performance Fiber-Reinforced Concrete. *ACI MATERIALS JOURNAL, 104*, 146-152.

Graybeal, B. A. (2007). Compressive Behavior of Ultra-High-Performance Fiber-Reinforced Concrete. *ACI MATERIALS JOURNAL, 104*(2).

Jiao, C., Sun, W., Huan, S., & Jiang, G. (2009). Behavior of steel fiber - Reinforced high-strength concrete at medium strain rate. *Frontiers of Architecture and Civil Engineering in China, 3*, 131-136. doi:10.1007/s11709-009-0027-0

Jo, B.-W., Shon, Y.-H., & Kim, Y.-J. (2001). The Evalution Of Elastic Modulus for Steel Fiber Reinforced Concrete. *Russian Journal of Nondestructive Testing, 37*(2), 152-161. doi:10.1023/A:1016780124443

Kazemi, S., & Lubell, A. (2012). Influence of Specimen Size and Fiber Content on Mechanical Properties of Ultra-High-Performance Fiber-Reinforced Concrete. *ACI MATERIALS JOURNAL, 109*, 675-684. doi:10.14359/51684165

Kim, D. J., Park, S.H., Ryu, G.S., & Koh, K.T. . (2011). Comparative flexural behavior of Hybrid Ultra High Performance Fiber Reinforced Concrete with different macro fibers. *Construction and Building Materials, 25*(11), 4144-4155.

Lavanya, S., Dattatreya, J., M.Neelamegam, & Seshagiri Rao, M. (2010). STUDY ON STRESS-STRAIN PROPERTIES OF REACTIVE POWDER CONCRETE UNDER UNIAXIAL COMPRESSION. *International Journal of Engineering Science and Technology, 2*.

Lavanya, S., J K, D., & Neelamegam, M. (2014). STRESS STRAIN BEHAVIOUR OF ULTRA HIGH PERFORMANCE CONCRETE UNDER UNIAXIAL COMPRESSION. *International Journal of Civil Engineering and Technology (IJCIET) 0976-6316, 5*, 187-194.

Lee, I. Complete Stress-Strain Characteristics of High Performance Concrete.

Lim, J. C., & Ozbakkaloglu, T. (2014). Stress-Strain Model for Normal- and Light-Weight Concretes under Uniaxial and Triaxial Compression. *Construction and Building Materials, 71*. doi:10.1016/j.conbuildmat.2014.08.050

Lu, Z.-H., & Zhao, Y.-G. (2010). Empirical Stress-Strain Model for Unconfined High-Strength Concrete under Uniaxial Compression. *Journal of Materials in Civil Engineering - J MATER CIVIL ENG, 22*. doi:10.1061/(ASCE)MT.1943-5533.0000095

Lubell, S. K. a. A. S. Influence of Specimen Size and Fiber Content on Mechanical Properties of Ultra-High-Performance Fiber-Reinforced Concrete. *ACI MATERIALS JOURNAL, 109*(6).

Maher KT, V. Y. (2016). Taking Ultra-High Performance Concrete to New Height – The Malaysian Experience. *Aspire the Concrete Bridge Magazine, Summer 2016*, 36-38.

Mansur, M. A., Chin, M., & Wee, T. (1999). Stress-Strain Relationship of High-Strength Fiber Concrete in Compression. *Journal of Materials in Civil Engineering - J MATER CIVIL ENG, 11*. doi:10.1061/(ASCE)0899-1561(1999)11:1(21)

Mindessb, G. C. a. S. (2000). Size Effect in Compression of High Strength Fibre Reinforced Concrete Cylinders Subjected To Concentric And Eccentric Loads. *Materials for Buildings and Structures*.

Nataraja, M., Dhang, N., & Gupta, A. P. (1999). *Stress–strain curves for steel-fiber reinforced concrete under compression* (Vol. 21).

Pierre-Claude Aitcin, B. M., Willliam D. Cook, and Denis Mitchell. (1994). Effects of Size and Curing on Cylinder Compressive Strength of Normal and High-Strength Concretes. *ACI MATERIALS JOURNAL, 91*(4), Title no. 91-M34.

Pierre Richard, M. C. (1995). COMPOSITION OF REACTIVE POWDER CONCREXES *Cement and Concrete Research, Vol. 25*.(7), 1501-1511.

Popovics, S. (1973). A NUMERICAL APPROACH TO THE COMPLETE STRESS-STRAIN CURVE OF CONCRETE. *Cement and Concrete Research, 3*, 583-599.

Shafieifar, M., Farzad, M., & Azizinamini, A. (2017). Experimental and numerical study on mechanical properties of Ultra High Performance Concrete (UHPC). *Construction and Building Materials, 156*, 402-411. doi:10.1016/j.conbuildmat.2017.08.170

Sobuz, H. R., Visintin, P., Mohamed Ali, M. S., Singh, M., Griffith, M. C., & Sheikh, A. H. (2016). Manufacturing ultra-high performance concrete utilising conventional materials and production methods. *Construction and Building Materials, 111*, 251-261. doi:10.1016/j.conbuildmat.2016.02.102

Suksawang, N., Wtaife, S., & Alsabbagh, A. (2018). Evaluation of Elastic Modulus of Fiber-Reinforced Concrete. *ACI MATERIALS JOURNAL, 115*. doi:10.14359/51701920

Toledo Filho, R. D., Koenders, E. A. B., Formagini, S., & Fairbairn, E. M. R. (2012). Performance assessment of Ultra High Performance Fiber Reinforced Cementitious Composites in view of sustainability. *Materials & Design (1980-2015), 36*, 880-888. doi:10.1016/j.matdes.2011.09.022

Wille K, T. N., Parra-Montesinos GJ. (2014). Fiber distribution and orientation in UHP-FRC beams and their effect on backward analysis. *Materials and Structures, 47(11)*, 1825–1838.

YI, J.-K. K. a. S.-T. (2002). Application of size effect to compressive strength of concrete members. *S¯adhan¯a, 27*, 467-484.

Yoo, D.-Y., & Yoon, Y.-S. (2016). A Review on Structural Behavior, Design, and Application of Ultra-High-Performance Fiber-Reinforced Concrete. *International Journal of Concrete Structures and Materials, 10*(2), 125-142. doi:10.1007/s40069-016-0143-x

Zhao-Hui Lu and Yan-Gang Zhao, M. A. (2010). Empirical Stress-Strain Model for Unconfined High-Strength Concrete under Uniaxial Compression. *JOURNAL OF MATERIALS IN CIVIL ENGINEERING © ASCE, 22(11)*, 1181-1186. doi:10.1061/ASCEMT.1943-5533.0000095